

Interstitial Fluid Pressure Correlates Clinicopathological Factors of Lung Cancer

Takeshi Mori, MD, PhD,¹ Takamasa Koga, MD,¹ Hidekatsu Shibata, MD, PhD,¹ Koei Ikeda, MD, PhD,¹ Kenji Shiraishi, MD, PhD,¹ Makoto Suzuki, MD, PhD,¹ and Ken-ichi Iyama, MD, PhD²

Purpose: Solid tumors show increased interstitial fluid pressure (IFP), which correlates to a number of pathophysiological features of tumors. There have been no reports on the usefulness of measuring IFP in lung cancer. The aim of this study was to examine the relationship between IFP and the clinicopathological characteristics of lung cancer.

Methods: IFP was measured prospectively in 215 patients with 219 lesions showing solid or part-solid appearance. Four patients with double lung cancer were excluded from the analysis, resulting in 211 patients with lung cancer being analyzed for the correlation between IFP and computed tomography (CT) appearance, size, Tumor-node-metastasis (TNM) classification, maximal standardized uptake value (SUVmax), histological type, tumor grade, pleural and vessel invasion, Ki-67 index, and recurrence-free survival (RFS). **Results:** The mean IFP was 8.5 mmHg; IFP was significantly correlated with the tumor size, SUVmax, TNM, vessel and pleural invasion, and Ki-67 index. Low IFP was associated with a better RFS compared to high IFP. Multivariate analysis did not select IFP as independent prognostic factor. In subgroup analysis of patients with adenocarcinoma, IFP was selected as independent one.

Conclusions: IFP correlates clinicopathological factors of lung cancer. IFP might be used as a prognostic factor for lung cancer.

Keywords: lung cancer, interstitial fluid pressure, clinicopathological factor

Introduction

Solid tumors generally show increased interstitial fluid pressure (IFP), which has been demonstrated to correlate with a number of pathophysiological features of tumors. Since an initial report by Young, et al in 1950,¹⁾ several

studies on IFP in solid tumors have been reported. Curti, et al. demonstrated that patients with melanoma or lymphoma who responded to chemotherapy showed progressive lowering of the tumor IFP,²⁾ and Tanaka, et al. reported that IFP might be a causal factor of tumor spread in hepatocellular carcinoma.³⁾ High tumor IFP has been found to correlate with a high recurrence rate and poor prognosis for patients with cervical cancer who receive radiation therapy,^{4,5)} and Yeo, et al. reported that IFP was a useful predictor of radiation therapy response for cervical cancer.⁶⁾ Moreover, the IFP in rectal cancer has been demonstrated to decrease after bevacizumab treatment.⁷⁾ These studies support a role for IFP as a prognostic factor for patients with solid tumors, with low IFP indicating a more favorable prognosis for patients with solid tumors who received radiation therapy, chemotherapy, and molecular targeted therapy. However, despite the numerous

¹Departments of Thoracic Surgery, Graduate School of Medical Sciences, Kumamoto University, Kumamoto, Kumamoto, Japan

²Department of Surgical Pathology, Kumamoto General Hospital, Yatsushiro, Kumamoto, Japan

Received: July 27, 2014; Accepted: September 27, 2014

Corresponding author: Takeshi Mori, MD, PhD. Department of Thoracic Surgery, Graduate School of Medical Sciences, Kumamoto University, 1-1-1 Honjo Chuo-ku, Kumamoto, Kumamoto 860-8556, Japan.

E-mail: morimori@fc.kuh.kumamoto-u.ac.jp

©2015 The Editorial Committee of *Annals of Thoracic and Cardiovascular Surgery*. All rights reserved.

reports on the usefulness of measuring IFP for these tumors, currently, there are no reports on the association between IFP and the prognosis and clinicopathological characteristics of lung cancer, with the exception of studies on human lung cancer xenografts grown in nude mice.^{8,9}

Previously, IFP was generally determined via the wick-in-needle or micropuncture technique.¹⁰⁾ However, a simple method for measuring IFP by using a polyurethane transducer-tipped catheter was recently developed,¹¹⁾ and we used this technique to measure the IFP of lung cancer.

The aims of this study were to develop a method to measure IFP for lung cancer showing solid or part-solid appearance on computed tomography (CT) scans and to examine the relationship between IFP and tumor aggressiveness of lung cancer.

Materials and Methods

Eligibility

The study protocol was approved by the Ethical Committee of Kumamoto University Hospital in May 2009. Informed consent was obtained from all the patients after discussing the risks and benefits of the study with their surgeons.

Patients

Between September 2009 and January 2013, 501 patients with 514 lung cancers underwent resection at our institute. Of these 514 lesions, 129 showing a pure ground-glass appearance on CT scans, 78 showing part-solid appearance of which the size of the solid part was <1 cm, and 14 showing pure solid appearance <1 cm were excluded, because it was difficult to ensure tumor localization for IFP measurement during the preliminary experiments (data not shown). In addition, seven lesions with cavities and six lesions treated with preoperative therapy such as chemoradiation, chemotherapy, and radiation were also excluded. Moreover, 61 lesions could not be measured for IFP because resection was performed while the microtip catheter was under repair or during the absence of the person measuring (T.M.) the IFP, resulting in 219 lesions in 215 patients being measured for IFP. Of these 215 patients, four patients who had two lung cancers were excluded from the analysis. As a result, 211 lesions in 211 patients were included in the analysis (**Table 1**). There were 139 men and 72 women with a mean age of 70 ± 9 years (median: 70 years; range: 39 years–87 years).

Measuring IFP of lung cancer

IFP was measured in the resected lung cancer specimens. First, the ends of the pulmonary artery and vein of the resected lung cancer, which had been closed via surgical stapler or ligation, were opened to remove remnant blood. Second, IFP was measured at the center of the tumor, as IFP is reported to be higher in the center than in the peripheral area of the tumor,¹²⁾ by using the 1Fr Mikro-Tip sensor catheter (model SPR-1000, Millar, Houston, Texas, USA) as described previously.¹¹⁾ The method of measuring IFP for lung cancer is summarized in **Fig. 1**.

Positron Emission Tomography-CT scanning

Sixteen patients did not show accumulation of 18F-fluorodeoxyglucose in the lesions; therefore, their maximal standard uptake value (SUVmax) was calculated as 0.

Pathological analysis

Hematoxylin and eosin staining and Victoria blue staining were performed for all sections to investigate the intratumoral lymphatic and vascular invasion as well as pleural involvement. Pleural involvement was classified as pI0, pI1, pI2, and pI3 (tumors within the subpleural lung parenchyma or superficially invading the pleural connective tissue beneath the elastic layer, tumors invading beyond the elastic layer, tumors invading the pleural surface, and tumors invading any component of the parietal pleura, respectively). The tumors were staged according to the criteria of the 7th edition of Tumor-node-metastasis (TNM) classification.¹³⁾

Immunohistochemical staining

Immunostaining was performed by the Dako envision system (Dako, Glostrup, Denmark). Antibodies for Ki-67 (monoclonal mouse antibody MIB-1, 1:50 dilution) and CD34 (monoclonal mouse antibody, NU-4A1, 1:50 dilution) were purchased from Dako (Denmark) and Nichirei bioscience (Tokyo, Japan), respectively. Sections of 4 μm were cut from the paraffin blocks, and immunostaining was performed with antigen-retrieval techniques as previously described.¹⁴⁾

Evaluation of immunohistochemical staining

Ki-67

The Ki-67 labeling index was measured by determining the percentage of cells with positive nuclei in >1000 tumor cells in >4 fields.¹⁵⁾ The mean number of tumor cell count was 1112 ± 114 .

Table 1 Patient characteristics

Sex	Number	Mean \pm SD (range)
Male	139 (66%)	
Female	72 (34%)	
Age (years)		70 \pm 9 (39–87)
Size (cm)		2.8 \pm 1.5 (1.0–7.9)
CT findings		
Solid	148 (70%)	
Part-solid	63 (30%)	
Size of the solid part (cm)		2.5 \pm 1.5 (1.0–7.9)
Pathological size (cm)		2.5 \pm 1.4 (0.6–8.6)
SUVmax (n = 191)		4.7 \pm 4.2 (0–18.7)

SD: standard deviation; CT: computed tomography; SUVmax: maximal standardized uptake value

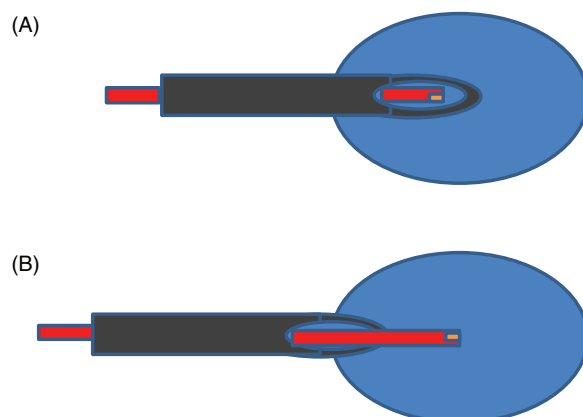


Fig. 1 Schema of the method used to measure the interstitial fluid pressure (IFP) of the tumors. (A) The ultraminiature transducer, SPR-1000, is introduced into the tumor in a protective metal guide (23-gauge needle). (B) The metal guide is slowly withdrawn while the sensor is introduced into the center of the tumor, where IFP is measured. In this study, IFP was measured by using resected specimens of lung cancer after remnant blood removal.

CD34 (Microvessel density)

The areas of highest microvessel density (MVD) were used for counting the microvessels. The average numbers of CD34-positive capillaries and small venules were carefully counted in 4 high-power fields.

Statistical analysis

The unpaired *t*-test was used to analyze the associations between IFP and sex, appearance on CT scans, histology (squamous cell carcinoma vs. other histological types), and vessel invasion. The relationship between IFP

and the following factors were analyzed by using the Spearman rank test: tumor grade, pleural invasion, and clinical/pathological TNM factors. The relationships between IFP and the following factors were analyzed by using the Pearson *r* test: age, clinical/pathological tumor size, size of the solid part on CT scans, SUVmax, Ki-67 index, and MVD. Receiver operating characteristics (ROC) curves were used to determine the cutoff value of IFP for recurrence. Estimated likelihood of events was calculated by using the Kaplan-Meier method. The log-rank test was used to compare differences between curves. Univariate and multivariate analyses were performed with Cox regression model. Statistical analysis was performed by using SPSS software (version 18; IBM SPSS Statistics, Chicago, Illinois, USA). All values in the text and tables are given as mean \pm standard deviation.

Results

Table 1 shows the patients' characteristics. On high resonance CT scans, lesions showing part-solid features were observed in 63 patients with adenocarcinoma, whereas solid lesions were observed in 148 patients. The long-axis diameter of the pulmonary nodules/masses was selected as the size of the lesions. The mean size of these 211 lesions observed on CT scans was 2.8 \pm 1.5 cm (range: 1.0 cm–7.9 cm), and the mean size of the solid part was 2.5 \pm 1.5 cm (range: 1.0 cm–7.9 cm). The mean pathological size of the lesions was 2.5 \pm 1.4 cm (range: 0.6 cm–8.6 cm). Twenty patients did not undergo positron emission tomography (PET), resulting in the relationship between IFP and SUVmax being examined in 191 patients. The mean SUVmax was 4.7 \pm 4.2 (0–18.7,

Table 2 Correlation between the interstitial fluid pressure (IFP) and clinicopathological factors

Factor	IFP (mean ± SD)	rho	r	p-value
CT findings				
Solid (n = 148)	9.8 ± 6.8			<0.001
Part-solid (n = 63)	5.5 ± 4.7			
Tumor size (CT)		0.309	<0.001	
Size of the solid part (CT)		-0.077	0.27	
Tumor size (pathological)		0.320	<0.001	
SUVmax (n = 191)		0.475	<0.001	
Histological types				
SqCC (n = 52)	10.3 ± 7.5			<0.008
non-SqCC (n = 159)	7.8 ± 6.1			
AD (n = 142)	7.7 ± 6.1			
AdSq (n = 10)	7.3 ± 3.8			
Others (n = 7)	11.2 ± 7.8			
Lymphatic vessel invasion				
ly- (n = 176)	7.7 ± 6.3			<0.001
ly+ (n = 35)	12.6 ± 6.2			
Vascular vessel invasion				
v- (n = 148)	7.2 ± 6.0			<0.001
v+ (n = 63)	11.6 ± 6.9			
Pleural invasion		0.272		<0.001
0 (n = 159)	7.5 ± 5.9			
1 (n = 28)	10.5 ± 7.5			
2 (n = 7)	10.2 ± 4.3			
3 (n = 17)	14.0 ± 8.1			
Grade		0.305		<0.001
1 (n = 95)	6.5 ± 4.8			
2 (n = 88)	9.7 ± 7.3			
3 (n = 26)	11.0 ± 6.9			
4 (n = 2)	20.5 ± 6.6			
Ki-67 index	25 ± 19	0.303		<0.001
MVD	12.8 ± 8.1	0.061		0.38

SD: standard deviation; rho: Spearman rho; r: Pearson r; CT: computed tomography; AD: adenocarcinoma; SqCC: squamous cell carcinoma; AdSq: adenosquamous carcinoma; others: other histological types of lung cancer (small cell lung cancer [n = 1], alpha-feto protein producing lung cancer [n = 1], carcinoid [n = 2], large cell carcinoma with neuroendocrine feature [n = 2], and mucoepidermoid carcinoma [n = 1]); MVD: microvascular density

n = 191). The tumors consisted of the following histological subtypes: adenocarcinoma, Squamous cell carcinoma, adenosquamous carcinoma, and others in 142, 51, 10, and 8 patients, respectively. The pathological tumor stages were T1aN0M0 in 75 patients, T1bN0M0 in 38 patients, T2aN0M0 in 48 patients, stage IIA in 19 patients, stage IIB in 6 patients, stage IIIA in 22 patients, stage IIIB in 1 patient, and stage IV in 2 patients.

The mean IFP of the 211 lesions was 8.5 ± 6.6 mmHg (range: 0 mmHg – 32.7 mmHg), and the mean IFP of the solid lesions was 9.8 ± 6.8 mmHg, which was significantly higher than that of the part-solid lesions (5.5 ± 4.7 mmHg;

$p <0.001$; **Table 2**). IFP correlated with the clinical/pathological size ($p <0.001$), but it did not correlate with the size of the solid part observed on CT scans (**Table 2**). The mean SUVmax of lung cancer observed on PET-CT scans was 4.7 ± 4.2 (**Table 1**), which showed significant correlation with the IFP ($r = 0.475$, $p <0.001$; **Table 2**, **Fig 2**).

The mean IFPs according to the histological types of lung cancer were as follows: 7.7 ± 6.1 mmHg in adenocarcinoma, 10.3 ± 7.5 mmHg in squamous cell carcinoma, and 7.3 ± 3.8 mmHg in adenosquamous carcinoma. The mean IFP of squamous cell carcinoma of the lung

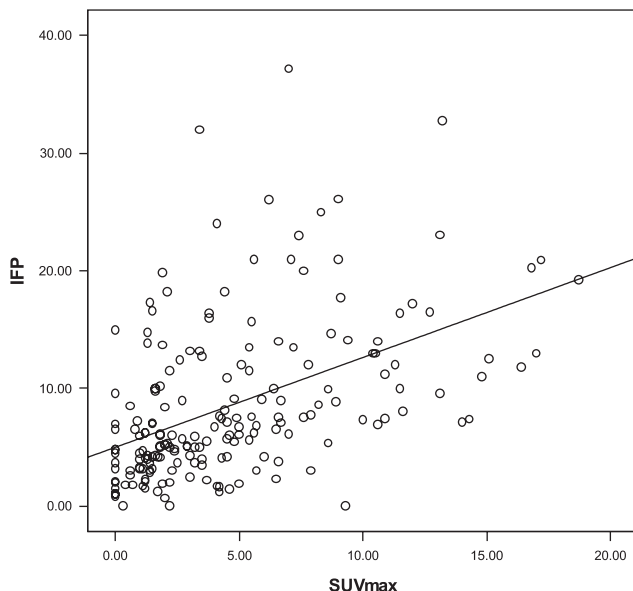


Fig. 2 Correlation between interstitial fluid pressure (IFP) and maximal standardized uptake value (SUVmax). SUVmax showed a significant correlation with the IFP ($r = 0.475$, $p < 0.001$).

was significantly higher than that of non-squamous cell carcinoma of lung cancer (7.8 ± 6.1 mmHg) ($p = 0.008$, **Table 2**).

Table 3 shows the correlation between the IFP and pathological TNM stage. Pathological N factor and stage as well as pathological T factor were significantly correlated with the IFP ($p < 0.001$ for all; **Table 3**). Clinical TNM was also significantly correlated with the IFP (data not shown). Moreover, vessel and pleural invasion and tumor grade showed significant correlations with the IFP ($p < 0.001$; **Table 2**). However, while the Ki-67 index was significantly correlated with IFP ($r = 0.303$, $p < 0.001$), the MVD did not (**Table 2**).

The optimal cut-off value of IFP was determined to be 7.4 mmHg using the ROC curve, which was associated with the sensitivity and specificity values of 0.74 and 0.61, respectively. Recurrence-free survival (RFS) in the low IFP group ($IFP \leq 7.4$ mmHg) was significantly better than that in the high IFP group ($IFP > 7.4$ mmHg). The 4-year RSF of the low and high IFP groups was 84 months and 70 months, respectively ($p = 0.001$, mean follow up period: 28 ± 11 months; range: 1–54 months; **Fig. 3**).

Table 4 shows univariate and multivariate analyses of factors influencing RFS. In multivariate analysis, lymphatic vessel invasion was selected as an independent prognostic factor influencing RFS (hazard ratio [HR]

Table 3 Correlation between the pathological TNM classification and interstitial fluid pressure (IFP)

	IFP (mmHg) (mean \pm SD)	Spearman rho	p-value
T			
T1a (n = 80)	6.9 ± 5.9	0.297	<0.001
T1b (n = 45)	6.5 ± 4.8		
T2a (n = 64)	10.6 ± 7.0		
T2b (n = 9)	13.9 ± 7.4		
T3 (n = 9)	13.3 ± 9.0		
T4 (n = 4)	6.1 ± 2.8		
N			
N0 (n = 177)	7.6 ± 6.2	0.356	<0.001
N1 (n = 19)	13.3 ± 6.3		
N2 (n = 19)	13.5 ± 6.3		
Stage			
IA (n = 121)	6.4 ± 4.4	0.359	<0.001
IB (n = 43)	10.6 ± 8.7		
IIA (n = 17)	11.9 ± 6.4		
IIB (n = 6)	12.7 ± 11.5		
IIIA (n = 20)	12.8 ± 6.5		
IIIB (n = 2)	9.3 ± 2.5		
IV (n = 2)	7.9 ± 8.0		

SD: standard deviation; TNM: Tumor-node-metastasis

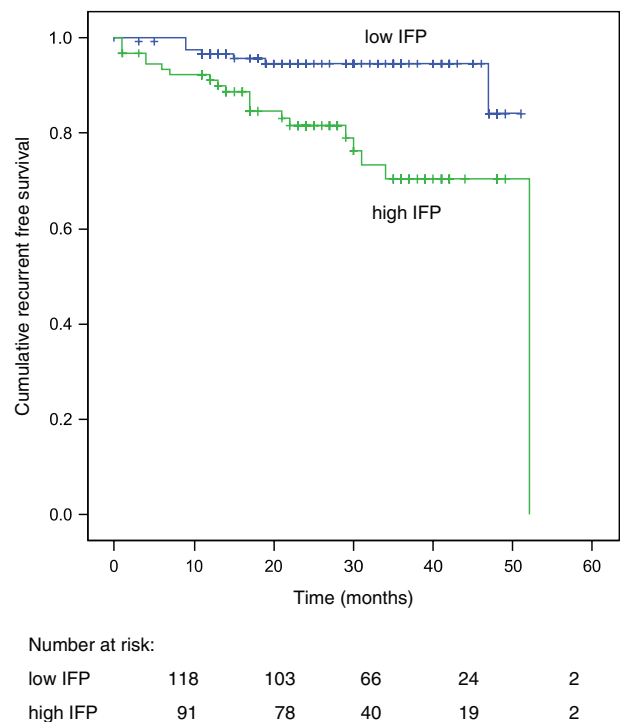


Fig. 3 Cumulative recurrence-free survival (RFS) curves for patients with lung cancer grouped according to the interstitial fluid pressure (IFP). The 4-year RFS rate in the low IFP group ($IFP \leq 7.4$ mmHg) was 84%, which was significantly higher than that in the high IFP group ($IFP > 7.4$ mmHg; 4-year RFS = 70%; $p = 0.001$).

Table 4 Univariate and multivariate analyses of factors influencing recurrent free survival

Factor	Univariate		Multivariate	
	HR (95% CI)	p	HR (95% CI)	p
Sex (female vs. male)	1.66 (0.69–3.98)	0.245		
Age	1.02 (0.98–1.07)	0.324		
Size (pathological)	1.04 (1.02–1.06)	<0.001	1.24 (0.98–1.07)	0.281
Size of part solid (CT)	1.01 (0.99–1.04)	0.307		
CT findings (part-solid vs. solid)	5.89 (1.39–24.94)	0.016	4.05 (0.46–35.95)	0.210
SUVmax	1.19 (1.10–1.29)	<0.001	0.97 (0.80–1.16)	0.703
IFP	1.07 (1.03–1.12)	0.001	1.06 (0.995–1.12)	0.074
Lymphatic vessel invasion	3.81 (2.39–6.07)	<0.001	2.77 (1.02–7.49)	0.045
Vascular vessel invasion	4.26 (2.37–7.66)	<0.001	1.42 (0.57–3.55)	0.454
Pleural invasion	1.94 (1.42–2.63)	<0.001	1.12 (0.71–1.78)	0.627
Grade	1.86 (1.15–3.01)	0.012	0.75 (0.33–1.71)	0.493
Ki-67	8.33 (1.30–53.3)	0.025	1.89 (0.06–58.88)	0.716
MVD	1.01 (0.98–1.06)	0.402		
T (pathological)	1.96 (1.53–2.57)	<0.001	1.13 (0.64–2.00)	0.676
N (pathological)	2.38 (1.47–2.86)	<0.001	0.74 (0.29–1.86)	0.514

HR: Hazard ratio; CI: confidence interval; CT: computed tomography; SUVmax: maximal standardized uptake value; IFP: interstitial fluid pressure; MVD: microvessel density

2.77, 95% confidence interval [CI] 1.02–7.49, $p=0.045$), IFP was not (HR 1.06, 95% CI 0.995–1.12, $p=0.074$). Subgroup analysis of the patients with adenocarcinoma showed that IFP (HR 1.06, 95% CI 1.04–1.45, $p=0.014$) and Ki-67 index (HR 4.22×10^5 , 95% CI 22.15–8.25 $\times 10^9$, $p=0.045$) were independent prognostic factors influencing RFS (**Table 5**).

Discussion

Since the report by Young, et al in 1950,¹⁾ a number of studies on the IFP of solid tumors have been reported.^{2–7)} These reports have shown that IFP correlates with the clinicopathological features of various solid tumors including melanoma, lymphoma, cervical cancer, and rectal cancer. Moreover, IFP has been reported to be a prognostic factor for the treatment outcomes of certain solid tumors,^{4–7)} such as radiation for cervical cancer^{4–6)} and bevacizumab treatment for rectal cancer.⁷⁾ However, to date, there have been no reports of IFP concerning lung cancer, with the exception of experiments of human lung cancer xenografts in nude mice.^{8,9)} To our knowledge, this study is the first report of IFP in clinical cases of lung cancer.

In this report, the IFP was correlated with the tumor size and pathological TNM stage of lung cancer. Similarly, Raut, et al. reported a correlation between the tumor size and the IFP in patients with refractory sarcoma.¹⁶⁾ Moreover, IFP

was correlated with both pathological N and T factors in this study, and, Dadiani, et al. had previously reported that high IFP induced fast draining of tumor cells to the lymphatic vessels in mice inoculated with human breast cancer cells.¹⁷⁾ IFP correlated with the tumor size, but it did not correlate with the size of solid part. IFP might not be created only by solid part of the tumor, but might be also created by ground glass part.

In the present study, the cut-off value of IFP for diagnosing recurrence of lung cancer was determined to be 7.4 mmHg by using the ROC curve. Interestingly, the low IFP group (IFP ≤ 7.4 mm Hg) showed better recurrence-free survival than the high IFP group (IFP >7.4 mmHg). Although multivariate analysis did not select IFP as independent prognostic factor, subgroup analysis of the patients with adenocarcinoma selected IFP as independent prognostic factor. These results, as well as those of the previous reports in other types of cancers,^{4–7)} support the use of IFP as a candidate novel prognostic factor for lung cancer.

Moreover, IFP was found to correlate with the Ki-67 index and SUVmax in this study. Watanabe, et al. reported that the SUV was correlated with the Ki-67 in clinical stage IA lung adenocarcinoma;¹⁴⁾ therefore, we speculate that IFP might be able to predict tumor aggressiveness of lung cancer similarly to 18F-fluorodeoxyglucose PET.

Table 5 Univariate and multivariate analyses of factors influencing disease free survival of the patients with adenocarcinoma

Factor	Univariate		p	Multivariate	
	HR (95% CI)			HR (95% CI)	p
Sex (female vs. male)	2.27 (0.69–7.50)	0.179			
Age	1.02 (0.96–1.09)	0.502			
Size (pathological)	1.04 (1.02–1.06)	<0.001	1.05 (0.31–9.81)	0.271	
Size of part solid (CT)	1.03 (1.00–1.54)	0.092	1.06 (0.99–1.13)	0.080	
CT findings (part-solid vs. solid)	4.79 (1.06–21.64)	0.042	0.55 (0.03–9.82)	0.685	
SUVmax	1.25 (1.08–1.45)	0.003	0.75 (0.45–1.25)	0.263	
IFP	1.14 (1.07–1.22)	<0.001	1.06 (1.04–1.40)	0.014	
Lymphatic vessel invasion	5.04 (2.22–11.43)	0.001	4.74 (0.25–91.58)	0.303	
Vascular vessel invasion	4.44 (2.17–9.08)	<0.001	0.66 (0.11–3.78)	0.636	
Pleural invasion	2.11 (1.38–3.25)	0.001	1.05 (0.29–3.48)	0.994	
Grade	3.09 (1.30–7.35)	0.011	1.50 (0.92–24.32)	0.776	
Ki-67	172.2 (3.93–7560)	0.008	422404 (22.15–8.25 × 10 ⁹)	0.010	
MVD	1.04 (0.96–1.13)	0.306			
T (pathological)	12.54 (1.74–3.71)	<0.001	1.91 (0.42–8.69)	0.404	
N (pathological)	2.76 (1.46–5.22)	0.002	0.74 (0.11–10.4)	0.954	

HR: Hazard ratio; CI: confidence interval; CT: computed tomography; SUVmax: maximal standardized uptake value; IFP: interstitial fluid pressure; MVD: microvessel density

Importantly, IFP in this study was measured after resection, not before resection. To puncture the lungs *in vivo* may cause lethal complications such as air embolism or pleural dissemination.¹⁸⁾ Even after thoracotomy, puncture of the lung has a possibility to cause such complications. Before this paper, there had been no reports supporting the benefit of measuring IFP for lung cancer; therefore, in this study, we measured the IFP only after resection.

In this study, the IFP did not show any correlation with the MVD, which differs from the findings of previous reports. Raut, et al. reported that the patients with refractory sarcoma demonstrated a decline in IFP and MVD after sorafenib treatment,¹⁵⁾ and Deng, et al. similarly reported that chemotherapy in mice bearing xenografts of A549 cells led to a decline in the IFP and MVD.¹⁹⁾ As mentioned in the Methods section, the IFP in this study was measured in resected specimens after remnant blood removal. There are a number of factors that contribute to the increased IFP in the solid tumor, including blood-vessel leakiness, vessel abnormalities, interstitial fibrosis, and contraction of the interstitial matrix.²⁰⁾ Therefore, the IFP in this study might be weakly influenced by blood flow and vessel factors, compared with the IFPs previously reported.^{1–9, 16, 19)}

This report has some limitations. First, the IFP in this study was measured only after resection of lung cancer; the IFP measured during CT-guided biopsy or before lung cancer resection might be different from that measured in this study. To examine this problem, a novel study in which IFP will be measured before and after lung cancer resection is being planned. Furthermore, this report did not include consecutive patients with lung cancer who underwent surgery at our institute, because of microtip catheter issues and absence of the IFP measurer.

Conclusion

In conclusion, the IFP of lung cancer with solid or part-solid appearance on CT scans measured after resection showed correlation with a number of clinicopathological factors. Low IFP in the tumors was associated with better recurrence-free survival than high IFP in the tumors; therefore, the IFP of lung tumors might be a novel prognostic factor for lung cancer.

Acknowledgements

This study was supported by, in part, Grant-in-Aid from the Ministry of Education, Culture, Sports, Science and Technology of Japan.

Disclosure Statement

All authors have no conflict of interest.

References

- 1) Young JS, Lumsden CE, Stalker AL. The significance of the tissue pressure of normal testicular and of neoplastic (Brown-Pearce carcinoma) tissue in the rabbit. *J Pathol Bacteriol* 1950; **62**: 313-33.
- 2) Curti BD, Urba WJ, Alvord WG, et al. Interstitial pressure of subcutaneous nodules in melanoma and lymphoma patients: changes during treatment. *Cancer Res* 1993; **53**: 2204-7.
- 3) Tanaka T, Yamanaka N, Oriyama T, et al. Factors regulating tumor pressure in hepatocellular carcinoma and implications for tumor spread. *Hepatology* 1997; **26**: 283-7.
- 4) Roh HD, Boucher Y, Kalnicki S, et al. Interstitial hypertension in carcinoma of uterine cervix in patients: possible correlation with tumor oxygenation and radiation response. *Cancer Res* 1991; **51**: 6695-8.
- 5) Milosevic M, Fyles A, Hedley D, et al. Interstitial fluid pressure predicts survival in patients with cervix cancer independent of clinical prognostic factors and tumor oxygen measurements. *Cancer Res* 2001; **61**: 6400-5.
- 6) Yeo SG, Kim JS, Cho MJ, et al. Interstitial fluid pressure as a prognostic factor in cervical cancer following radiation therapy. *Clin Cancer Res* 2009; **15**: 6201-7.
- 7) Willett CG, Boucher Y, di Tomaso E, et al. Direct evidence that the VEGF-specific antibody bevacizumab has antivascular effects in human rectal cancer. *Nat Med* 2004; **10**: 145-7.
- 8) Vlahovic G, Rabbani ZN, Herndon JE, et al. Treatment with Imatinib in NSCLC is associated with decrease of phosphorylated PDGFR-beta and VEGF expression, decrease in interstitial fluid pressure and improvement of oxygenation. *Br J Cancer* 2006; **95**: 1013-9.
- 9) Lin BQ, Zeng ZY, Yang SS, et al. Dietary restriction suppresses tumor growth, reduces angiogenesis, and improves tumor microenvironment in human non-small-cell lung cancer xenografts. *Lung Cancer* 2013; **79**: 111-7.
- 10) Aukland K, Reed RK. Interstitial-lymphatic mechanisms in the control of extracellular fluid volume. *Physiol Rev* 1993; **73**: 1-78.
- 11) Ozerdem U, Hargens AR. A simple method for measuring interstitial fluid pressure in cancer tissues. *Microvasc Res* 2005; **70**: 116-20.
- 12) Boucher Y, Baxter LT, Jain RK. Interstitial pressure gradients in tissue-isolated and subcutaneous tumors: implications for therapy. *Cancer Res* 1990; **50**: 4478-84.
- 13) Goldstraw P, Crowley J, Chansky K, et al. The IASLC Lung Cancer Staging Project: proposals for the revision of the TNM stage groupings in the forthcoming (seventh) edition of the TNM Classification of malignant tumours. *J Thorac Oncol* 2007; **2**: 706-14.
- 14) Watanabe K, Nomori H, Ohtsuka T, et al. [F-18]Fluorodeoxyglucose positron emission tomography can predict pathological tumor stage and proliferative activity determined by Ki-67 in clinical stage IA lung adenocarcinomas. *Jpn J Clin Oncol* 2006; **36**: 403-9.
- 15) Martin B, Paesmans M, Mascaux C, et al. Ki-67 expression and patients survival in lung cancer: systematic review of the literature with meta-analysis. *Br J Cancer* 2004; **91**: 2018-25.
- 16) Raut CP, Boucher Y, Duda DG, et al. Effects of sorafenib on intra-tumoral interstitial fluid pressure and circulating biomarkers in patients with refractory sarcoma (NCI 6948). *PLoS ONE* 2012; **7**: e26331.
- 17) Dadiani M, Kalchenko V, Yosepovich A, et al. Real-time imaging of lymphogenic metastasis in orthotopic human breast cancer. *Cancer Res* 2006; **66**: 8037-41.
- 18) Wu CC, Maher MM, Shepard JA. Complications of CT-guided percutaneous needle biopsy of the chest: prevention and management. *AJR Am J Roentgenol* 2011; **196**: W678-82.
- 19) Deng PB, Hu CP, Xiong Z, et al. Treatment with EGCG in NSCLC leads to decreasing interstitial fluid pressure and hypoxia to improve chemotherapy efficacy through rebalance of Ang-1 and Ang-2. *Chin J Nat Med* 2013; **11**: 245-53.
- 20) Heldin CH, Rubin K, Pietras K, et al. High interstitial fluid pressure – an obstacle in cancer therapy. *Nat Rev Cancer* 2004; **4**: 806-13.